

REAPPRAISAL OF THE $k - \bar{\epsilon}$ MODEL CONSTANTS FOR THE WAKE OF A CIRCULAR CYLINDER

S. L. Tang

Institute for Turbulence-Noise-Vibration Interaction and Control,
Harbin Institute of Technology (Shenzhen), Shenzhen, 518055, P. R. China
Email: shunlin.tang88@gmail.com

L. Djenidi

School of Engineering, University of Newcastle, NSW 2308, Australia

R. A. Antonia

School of Engineering, University of Newcastle, NSW 2308, Australia

Y. Zhou

Institute for Turbulence-Noise-Vibration Interaction and Control, Shenzhen Graduate School,
Harbin Institute of Technology, Shenzhen, 518055, P. R. China

ABSTRACT

Starting with the N-S equations, Tang *et al.* (2015b) have derived an analytical expression of C_{ϵ_2} along the centreline in the far-wake of a circular cylinder and found that the value of C_{ϵ_2} differs markedly from the standard value of 1.92. This present study, in which we examine the effect of the mean shear on C_{ϵ_2} in regions away from the flow centreline, complements and extends our earlier examination of C_{ϵ_2} in this flow (Tang *et al.*, 2015b). Further, an analytical expression of C_{ϵ_1} is also derived from the N-S equations. The numerical value of C_{ϵ_1} is significantly smaller than the commonly used value of 1.44. Using these "new" values of C_{ϵ_2} and C_{ϵ_1} as new model constants in the $k - \bar{\epsilon}$ turbulence model, we find that the velocity defect U_d and the half-width of the far-wake L_0 agree reasonably well with the experimental data. When the calculation is based on the standard model constants, there is significant departure from the experimental data.

Introduction

The $k - \bar{\epsilon}$ turbulence model (k and $\bar{\epsilon}$ are the mean turbulent kinetic energy and its dissipation rate; the overbar denotes time averaging), is widely used in standard Computational Fluid Dynamics (CFD) simulations. For example, George *et al.* (2001) pointed out that it *accounts for about 95 % or more of the industrial use at present*. The main reason for its success is because CFD based on the $k - \bar{\epsilon}$ model is easy to implement and relatively less time and storage consuming than, for example, CFD based on the Reynolds stress turbulence models. Also, even though the values of

the (recommended) "standard" values of the model constants (Jones & Launder, 1972; Launder & Sharma, 1974) are not universal, the results provide the engineers with enough accuracy for a first order analysis in many flows. Since Jones & Launder's (Jones & Launder, 1972) paper, relatively little progress has been made on by and large ad-hoc calibration of the model constants. Indeed, the values of the model coefficients are obtained by imposing some constraints on the models when applied to relatively simple flows. For example, decaying homogeneous isotropic turbulence (HIT), or its surrogate, decaying grid turbulence ($\bar{\epsilon} = \partial k / \partial t$), turbulent channel flow (log law region) and homogenous shear flow (region where $\bar{\epsilon} / P_k \simeq \text{constant}$, P_k is the production of k) have been used to derive numerical values of the model constants in the transport equation of $\bar{\epsilon}$. Also, the model constants are "adjusted" until the predicted quantities (*e.g.* mean velocity, friction coefficient, near wall behaviour of $\bar{\epsilon}$) of a "reference" flow agree with their experimental and/or direct numerical simulation (DNS) counterparts. An example is the introduction of near-wall functions in the $k - \bar{\epsilon}$ turbulence model, which has led to several low Reynolds number $k - \bar{\epsilon}$ proposals (Launder & Sharma, 1974; Reynolds, 1976; Lam & Bremhorst, 1981; Chien, 1982; Hwang & Lin, 1998). Finally, techniques from the renormalization group theory have also been used to derive model constants for the $k - \bar{\epsilon}$ model (Yakhot & Orszag, 1986; Zhou *et al.*, 1997; Smith & Woodruff, 1998).

Regardless of the approach used to obtain the numerical values of the model coefficients, these values must conform to solutions of the Navier-Stokes equation for any particular flow. This is clearly a difficult task because of the

many free constants used in the turbulence models. The focus of the present work is on the modelled transport equation for $\bar{\epsilon}$, and in particular the constants C_{ϵ_1} and C_{ϵ_2} ; the latter involves modelling the balance between the production due to stretching of $\bar{\epsilon}$ and its destruction through the action of viscosity while the former involves modelling the source term (or production term). Already, [Tang et al. \(2015b\)](#) proposed an expression for C_{ϵ_2} on the centreline of a far-wake. Here, we extend their analysis to the regions away from the centreline and the expression for C_{ϵ_1} . Finally, we will use these "new" values of C_{ϵ_2} and C_{ϵ_1} as new model constants in the $k - \bar{\epsilon}$ turbulence model to carry out the simulation to check their validity.

Theoretical considerations

The modelled equation of $\bar{\epsilon}$ is (see for example [Pope \(2000\)](#))

$$\frac{d\bar{\epsilon}}{dt} = \frac{\partial}{\partial x_j} \left(\frac{\nu_T}{\sigma_\epsilon} \frac{\partial \bar{\epsilon}}{\partial x_j} \right) + C_{\epsilon_1} \frac{P_k \bar{\epsilon}}{k} - C_{\epsilon_2} \frac{\bar{\epsilon}^2}{k} \quad (1)$$

with

$$\frac{d\bar{\epsilon}}{dt} = \frac{\partial \bar{\epsilon}}{\partial t} + U_j \frac{\partial \bar{\epsilon}}{\partial x_j}, \quad (2)$$

where C_{ϵ_1} , C_{ϵ_2} and σ_ϵ are model constants to be determined and ν_T is the turbulent viscosity (or eddy viscosity). The first term on the right side of (1) represents the turbulent diffusion of $\bar{\epsilon}$, where a gradient-type model is adopted (ν_T/σ_ϵ is the turbulent Prandtl number). The second term represents a source term (or production) whose form is similar to its turbulent kinetic energy counterpart. The third term is a sink term which models the balance between the production due to stretching of $\bar{\epsilon}$ and its destruction through the action of viscosity. [Davidov \(1961\)](#) and later [Harlow & Nakayama \(1967, 1968\)](#) were the first to propose a modelled equation for the $\bar{\epsilon}$ -equation. However, [Jones & Launder \(1972\)](#) were arguably the first to propose what is regarded as the *standard* $k - \bar{\epsilon}$ model, even though the model constants used in the current $k - \bar{\epsilon}$ models are those proposed by [Launder & Sharma \(1974\)](#), viz.

$$C_{\epsilon_1} = 1.44, \quad C_{\epsilon_2} = 1.92, \quad \sigma_\epsilon = 1.3. \quad (3)$$

As mentioned in the Introduction, the numerical values of these constants have been obtained either by requiring the model to recover some basic physical properties of canonical flows such as grid turbulence, a homogeneous shear flow, wall flows ([Launder & Sharma, 1974](#)) or by using the Renormalization-Group theory (e.g. [Yakhot & Orszag \(1986\)](#) who obtained 1.42, 1.68 and 0.719 for C_{ϵ_1} , C_{ϵ_2} and σ_ϵ , respectively).

Scale-by-scale energy budget

We first apply a self-preservation analysis to the scale-by-scale energy budget equation or transport equation for $(\delta q)^2$; $(\delta q)^2 = (\delta u)^2 + (\delta v)^2 + (\delta w)^2$, where $\delta \alpha$ is the velocity increment $\delta \alpha = \alpha(x+r) - \alpha(x)$ between two points separated by a distance r along x , the flow direction; α

stands for either u , v , or w , v and w being velocity fluctuations in the y and z directions respectively. This equation can be expressed as:

$$-\frac{1}{r^2} \int_0^r s^2 [U \frac{\partial (\delta q)^2}{\partial x}] ds - \frac{2}{r^2} \int_0^r s^2 [\frac{\partial v (\delta q)^2}{\partial y} + \frac{\partial w (\delta q)^2}{\partial z}] ds - \delta u (\delta q)^2 + 2\nu \frac{\partial}{\partial r} (\delta q)^2 = \frac{4}{3} \bar{\epsilon} r \quad (4)$$

in the two-dimensional turbulent wake. The first and second terms in the second line of Eq. (4) represent the energy transfer and viscous diffusion of energy, respectively. The three terms in the first line are the advection, diffusion, and production terms respectively, which account for the inhomogeneity or non-stationarity associated with the large scales. At large r , Eq. (4) reduces to the one-point energy budget equation, while in the limit $r \rightarrow 0$, it reduces to the one-point transport equation of $\bar{\epsilon}$. For example, on the centreline of the far-wake of a circular cylinder, where the production is negligible ([Tang et al., 2015b](#)), the latter is (further assuming local isotropy)

$$\underbrace{-U \frac{\partial \bar{\epsilon}_{iso}}{\partial x}}_{Advection} - \underbrace{15 \frac{\partial \overline{u_2 \epsilon_1}}{\partial y}}_{Diffusion} = \frac{7}{3\sqrt{15}} \frac{\bar{\epsilon}_{iso}^{3/2}}{v^{1/2}} \left[S + 2 \frac{G}{R_\lambda} \right]. \quad (5)$$

(in the rest of the paper, u_1 , u_2 , and u_3 are used interchangeably with u , v , w ; similarly for x_1 , x_2 , x_3 and x , y , z) where S (<0) is the skewness of $\partial u/\partial x$

$$S = \frac{(\partial u/\partial x)^3}{(\partial u/\partial x)^2^{3/2}}, \quad (6)$$

G is the non-dimensional enstrophy destruction coefficient of $\bar{\epsilon}$

$$G = \frac{\overline{(\partial^2 u/\partial x^2)^2}}{(\partial u/\partial x)^2}, \quad (7)$$

and R_λ is the Taylor microscale Reynolds number

$$R_\lambda = \frac{\overline{u^2}^{1/2} \lambda}{\nu}, \quad (8)$$

where $\lambda = \overline{u^2}^{1/2} / (\partial u/\partial x)^2^{1/2}$ is the Taylor microscale. In Eq. (5), $\epsilon_1 = 2\nu \left(\frac{\partial u_1}{\partial x_1} \right)^2$ represents one component of the instantaneous energy dissipation rate ϵ

It can be shown that, on the centreline of the far-wake, the equation for $\bar{\epsilon}$ can be reduced to ([Tang et al., 2015b](#)).

$$S + 2 \frac{G}{R_\lambda} = \frac{C}{R_\lambda}, \quad (9)$$

when the self-preservation requirements for Eq. (4) are introduced in Eq. (5). Note that, along the centreline of the far-wake, $C = \frac{90}{7(1+2R)R_\epsilon} + 1.9$, where $R_\epsilon = \bar{\epsilon}_{iso}/\bar{\epsilon}$ and $R = \overline{v^2}/\overline{u^2} \approx \overline{w^2}/\overline{u^2}$ which account for the small-scale and large-scale anisotropy respectively ([Tang et al., 2015b](#)).

The analytical expressions for the constant C_{ε_2} in the far-wake can be easily determined by identifying the terms between the modelled equation (1) and each of the exact equations for $\bar{\varepsilon}$. Namely, combining (1) and (5), and after trivial manipulations, leads to

$$C_{\varepsilon_2} = \frac{7}{90} R_{\varepsilon}^2 (1 + 2R) (SR_{\lambda} + 2G). \quad (10)$$

Now, substituting Eq. (9) into Eq. (10) leads to

$$C_{\varepsilon_2} = \frac{7}{90} (1 + 2R) C. \quad (11)$$

Using $C = \frac{90}{7(1+2R)R_{\varepsilon}} + 1.9$ in (11), we obtain $C_{\varepsilon_2} = R_{\varepsilon} + \frac{7}{90} C_d R_{\varepsilon}^2 (1 + 2R)$. This and other expressions for C_{ε_2} are given in Table 1. Note that the expressions for C_{ε_2} in grid turbulence (e.g. Pope (2000); George *et al.* (2001)) and along the axis in far-field of a round jet (Thiesset *et al.*, 2014) have been reported previously. To date, only the grid-turbulence expression of C_{ε_2} has been used. It is evident from the various forms of C_{ε_2} (Table 1) that one cannot expect the grid turbulence value of C_{ε_2} to apply to other flows. This is evident from Table 1 which implies that the value of C_{ε_2} in each flow must be consistent with its expression for that flow.

Focus on the wake

Note that the expressions for C_{ε_2} in Table 1 for the jet and wake only apply to the flow centreline. We now focus only on the wake and specifically on the variations of C_{ε_2} and C_{ε_1} in the regions away from the flow centreline. With regard to C_{ε_2} , Fig. 1 shows the distribution of C_{ε_2} , as a function of y/L_0 (a detailed description of the measurements is given in Lefeuvre *et al.* (2014); $R_d = U_{\infty} d / \nu$ is 1400 and the corresponding R_{λ} is about 40 on the centreline). It can be seen from this figure that there is a weak dependence of C_{ε_2} on y/L_0 in the region close to the flow centreline. In particular, $C_{\varepsilon_2} \approx 1.60$ at $y/L_0 = 0$, which is in good agreement with the calculation using the expression in Table 1 for the wake. Also shown in this figure are the distribution of $(U_{\infty} - U)/U_d$, which shows that the range $y/L_0 < 0.5$ may be considered as the main region of the flow. Namely, at this R_d ($=1400$), a proper value for C_{ε_2} should be about 1.6; later, we will choose $C_{\varepsilon_2} \approx 1.55$ for a slightly higher R_d ($=2000$) for testing.

Now, we examine the dependence of C_{ε_1} , which involves modelling of the source term (or production term), on y/L_0 . From Eqs. (4) and (1), we can write the expression for C_{ε_1} as

$$\lim_{r \rightarrow 0} \frac{2}{r^2} \int_0^r s^2 \left[\frac{\partial U}{\partial y} \overline{(\delta u)(\delta v)} \right] ds / r^3 \equiv C_{\varepsilon_1} \frac{P_k \bar{\varepsilon}}{k}, \quad (12)$$

which, after trivial manipulations, leads to

$$C_{\varepsilon_1} = \frac{7\nu \frac{\partial u}{\partial x} \frac{\partial v}{\partial x} \overline{q^2}}{\bar{\varepsilon} \overline{uv}}. \quad (13)$$

If we assume self-preservation in the wake, C_{ε_1} can be normalized by the maximum defect velocity U_d and the half-

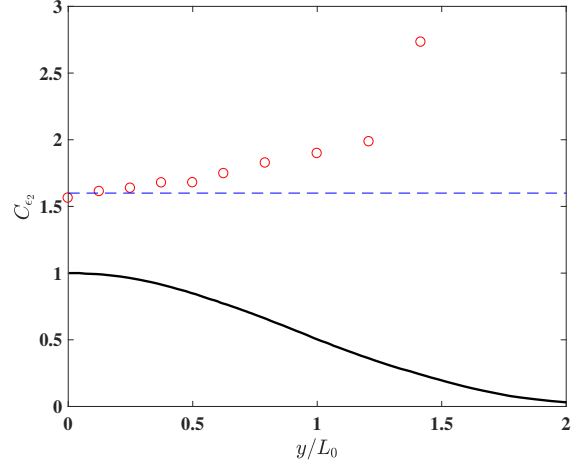


Figure 1. Dependence of C_{ε_2} on y/L_0 in the far-wake ($R_{\lambda} = 40$ on the centreline). The black curve: $(U_{\infty} - U)/U_d$ Browne *et al.* (1987). The dashed line: 1.60.

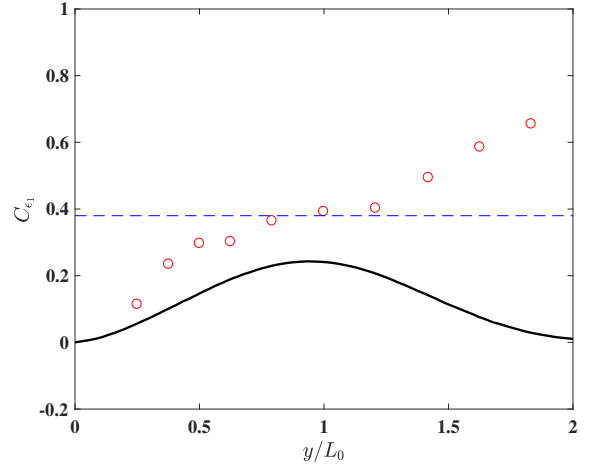


Figure 2. Dependence of C_{ε_1} on y/L_0 in the far-wake. The black curve: production of k , normalized by U_d and L_0 (Browne *et al.*, 1987). The dashed line: 0.38.

width of the wake L_0 , viz.

$$C_{\varepsilon_1} = \overline{\varepsilon_2^+} \overline{\varepsilon^+} \frac{q^{+2}}{uv^+}, \quad (14)$$

where the superscript $+$ denotes normalisation by U_d and L_0 ; $\overline{\varepsilon_2^+} = 7\nu \frac{\partial u}{\partial x} \frac{\partial v}{\partial x} \frac{L_0}{U_d^3}$. Note that each term in Eq. (14) should be a constant for a given y/L_0 . Fig. 2 shows the distribution of C_{ε_1} , as a function of y/L_0 , obtained with the same data as Fig. 1. Also shown in this figure is the production of k . Interestingly, in the region close to $y/L_0 \approx 1$ where the production term is large, C_{ε_1} is approximately constant, with a value of about 0.38. Since C_{ε_1} is basically the modelling of the production term, a proper value for C_{ε_1} should be about 0.38; we will use this "new" value, together with the "new" value for C_{ε_2} obtained above, to carry out a check of their validity.

Table 1. Expressions of C_{ε_2} in various turbulent flows.

$C_{\varepsilon_2} = \frac{(n-1)}{n}, n \leq -1$	decaying grid turbulence
$C_{\varepsilon_2} = \frac{(1+2R)}{2+R}$	along axis in far-field of a round jet
$C = \frac{90}{7(1+2R)R_\varepsilon} + 1.9$	centreline of the far-wake

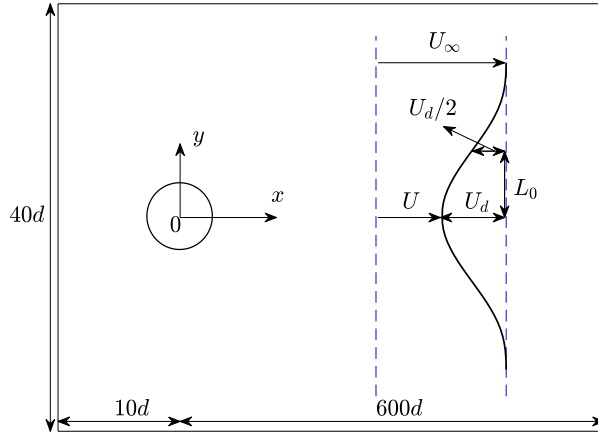


Figure 3. Schematic computational domain and coordinate axis. U is the mean velocity; U_∞ is the free stream velocity; U_d is the maximum velocity defect; L_0 is the half-width of the wake. Note that U and U_d are arbitrarily shown on the centreline.

Numerical validation

In order to validate the 'new' values obtained from N-S equations, we employ a commercial code, ANSYS-Fluent, for the simulations. The free-stream velocity U_∞ is 10.6 m/s and the cylinder diameter d is 3 mm. The corresponding R_d is 2000. The computational domain for the cylinder wake extends 10 and 600 diameters upstream and downstream from the cylinder centre respectively. A schematic diagram of the computational domain is shown in Fig. 3. Fig. 4 shows the downstream evolution of the velocity defect U_d and half-width of the wake L_0 at $R_d = 2000$. The red and blue curves are calculated using $k - \bar{\varepsilon}$ models with standard model constants ($C_{\varepsilon_1} = 1.44$, $C_{\varepsilon_2} = 1.92$) and 'new' constants obtained from N-S equations ($C_{\varepsilon_1} = 0.38$, $C_{\varepsilon_2} = 1.55$) respectively, while the other model constants are the same as in the standard $k - \bar{\varepsilon}$ models. The experimental data at the same R_d are reproduced from Tang *et al.* (2015a). Also shown are the experimental data of Aronson & Lofdahl (1993) at comparable R_d ($=1840$). U_d and L_0 agree reasonably well with the experimental data when the "new" values of C_{ε_2} and C_{ε_1} are used. However, when the calculation is based on the standard model constants, there is significant departure from the experimental data.

1 Conclusions

In this paper, we reappraise the constants C_{ε_2} and C_{ε_1} in the $k - \bar{\varepsilon}$ turbulence model. We first examine the effect of the mean shear on C_{ε_2} in regions away from the flow centreline, which complements and extends our earlier exami-

nation of C_{ε_2} in this flow. Further, an analytical expression of C_{ε_1} is also derived from the N-S equations. The numerical value of C_{ε_1} (≈ 0.38) is significantly smaller than the commonly used value of 1.44. Using these "new" values of C_{ε_2} and C_{ε_1} as new model constants in the $k - \bar{\varepsilon}$ turbulence model, we find that U_d and L_0 agree reasonably well with the experimental data, whereas there is significant departure from the experimental data when the calculation is based on the standard model constants.

Acknowledgements

SL Tang wishes to acknowledge support given to him from NSFC through grant 11702074. YZ wishes to acknowledge support given to him from NSFC through grants 11632006 and 91752109.

REFERENCES

- Aronson, D. & Lofdahl, L. 1993 The plane wake of a cylinder: Measurements and inferences on turbulence modeling. *Phys. Fluids* **5**, 1433.
- Browne, L. W., Antonia, R. A. & Shah, D. A. 1987 Turbulent energy dissipation in a wake. *J. Fluid Mech.* **179**, 307–326.
- Chien, K.Y. 1982 Predictions of channel and boundary-layer flows with a low-Reynolds-number model. *AIAA J.* **20**, 33–38.
- Davidov, B. I. 1961 On the statistical dynamics of an incompressible turbulent fluid. *Dokl. Akad. Nauk S.S.S.R.* **136**, 47–50.
- George, W. K., Wang, H., Wollblad, C. & Johansson, T. G. 2001 'homogeneous turbulence' and its relation to realizable flows. *14th Australasian Fluid Mechanics Conference, Melbourne* pp. Adelaide University, Adelaide, Australia.
- Harlow, F.H. & Nakayama, P.I. 1967 Turbulence transport equations. *Phys. Fluids* **10**, 2323–2323.
- Harlow, F.H. & Nakayama, P.I. 1968 Transport of turbulence energy decay rate. *Los Alamos Sci. Lab (Univ. of California) Report LA-3854*.
- Hwang, C.B. & Lin, C.A. 1998 Improved low-Reynolds $k - \bar{\varepsilon}$ model based on direct numerical simulation data. *AIAA J.* **36**, 38–43.
- Jones, W. P. & Launder, B. E. 1972 The prediction of laminarization with a two-equation model of turbulence. *Int. J. Heat Mass Transfer* **15**, 301–314.
- Lam, C.K.G. & Bremhorst, K.A. 1981 Modified for of $k - \bar{\varepsilon}$ model for predicting wall turbulence. *ASME Jnl. fluids Eng.* **103**, 456–460.
- Launder, B. E. & Sharma, B. I. 1974 Application of the energy-dissipation model of turbulence to the calculation of flow near a spinning disc. *Lett. Heat Mass Transfer* **1**, 131–138.
- Lefevre, N., Djenid, L., Antonia, R. A. & Zhou, T. 2014

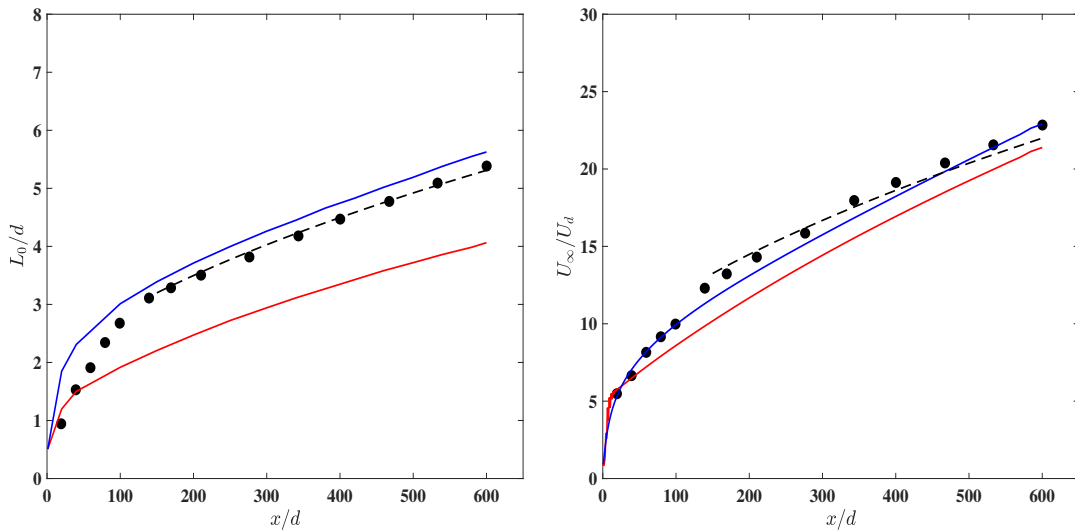


Figure 4. Downstream evolution of the velocity defect U_d and half-width of the wake L_0 at $R_d = 2000$. ●, experimental data (Tang *et al.*, 2015a); red and blue curves are calculated using $k-\bar{\epsilon}$ models with standard model constants ($C_{\epsilon_1} = 1.44$, $C_{\epsilon_2} = 1.92$) and 'new' constants obtained from N-S equations ($C_{\epsilon_1} = 0.38$, $C_{\epsilon_2} = 1.55$) respectively. Note that other model constants are the same as in the standard $k-\bar{\epsilon}$ models. Also shown are the experimental data of Aronson & Lofdahl (1993) at comparable R_d (=1840, black dashed line).

Turbulent kinetic energy and temperature variance budgets in the far-wake generated by a circular cylinder. *19th Australasian Fluid Mechanics Conference*.

Pope, S. B. 2000 Turbulent flows. Cambridge University Press.

Reynolds, W.C. 1976 Computation of turbulent flows. *Ann. Rev. Fluid Mech.* **8**, 183–208.

Smith, L.M. & Woodruff, S.L. 1998 Renormalization group analysis of turbulence. *Ann. Rev. Fluid Mech.* **30**, 275–310.

Tang, S. L., Antonia, R. A., Djenidi, L. & Zhou, Y. 2015a Complete self-preservation along the axis of a circular cylinder the far-wake. *J. Fluid Mech.* **786**, 253–274.

Tang, S. L., Antonia, R. A., Djenidi, L. & Zhou, Y. 2015b

Transport equation for the isotropic turbulent energy dissipation rate in the far-wake of a circular cylinder. *J. Fluid Mech.* **784**, 109–129.

Thiesset, F., Antonia, R. A. & Djenidi, L. 2014 Consequences of self-preservation on the axis of a turbulent round jet. *J. Fluid Mech.* **748** (R2).

Yakhot, V. & Orszag, S.A. 1986 Renormalization group analysis of turbulence: 1. basic theory. *Jnl. Sci. Comp.* **1**, 3–51.

Zhou, Y., McComb, W.D. & Vahal, G. 1997 Renormalization group (RG) in turbulence: Historical and comparative perspective. *ICASE report. No.97-36*, NACA CR-201728.